ELSEVIER

Biophysical Chemistry 99 (2002) 169–179

Biophysical Chemistry

www.elsevier.com/locate/bpc

Lysozyme viscoelastic matrices in tetramethylurea/water media: a small angle X-ray scattering study

Marcelo A. da Silva[a], Rosângela Itri[b], Elizabeth P.G. Arêas[a,*]

[a]*Departamento de Química Fundamental, Instituto de Química, Universidade de São Paulo, Caixa Postal 26077, CEP 05513-970, São Paulo, SP, Brazil*

[b]*Departamento de Física Aplicada, Instituto de Física, Universidade de São Paulo, Caixa Postal 66318, CEP 05515-970, São Paulo, SP, Brazil*

Received 3 May 2002; received in revised form 5 June 2002; accepted 5 June 2002

Abstract

Semi-solid viscoelastic matrices produced out of lysozyme in organic/aqueous media [tetramethylurea (TMU)/water] were characterized by small angle X-ray scattering (SAXS). The scattering curves were modeled in their form and interference factors. Radii of gyration of scattering particles were found to undergo a dramatic increase from 14 Å in water to approximately 44 Å in the matrices. Average correlation distances $d=155$ Å were consistently verified for the scattering particles in the matrices, irrespective of solvent composition (in the $0.6 \leq w_{TMU} \leq 0.8$ range), in contrast to what is observed in water ($d=62$ Å). At $w_{TMU}=0.9$, however, a slight increase in R_g (to $R_g=49$ Å) leads to interdigitation with the apolar prevailing medium of the matrix leading to the loss of the interference effect. Low dimensionality derived from the modeling procedure could be taken to indicate mass fractal character of the unfolded species, although polydispersion of samples could also have some contribution to that result. Despite the very significant shape distortion of the unfolded protein forms in the matrices, they still retain considerable globular character, as indicated by the Kratky plots obtained. The morphological results obtained in this work are compatible with the dynamical behavior displayed by the systems.

Keywords: Lysozyme; Small angle X-ray scattering; Rheology; Viscoelasticity; Protein networks; Fractals

1. Introduction

Our interest in approaching structural issues related to protein in organic media evolved from an original observation of remarkable viscoelastic features in protein systems that were otherwise perfect Newtonian fluids (when dispersed in aqueous media) [1]. The peculiar rheological behavior was first noticed in lysozyme dissolved in tetramethylurea (TMU)/water, for certain particular conditions of solvent composition [1]. Subsequent investigations widened the comprehension of aspects related to the phenomenon, confirming an inversion in the microconfiguration of the binary systems as the driving force for the protein folding

*Corresponding author. Tel.: +55-11-3091-2165; fax: +55-11-3815-5579.

E-mail address: epgareas@usp.br (E.P. Arêas).

0301-4622/02/$ - see front matter © 2002 Elsevier Science B.V. All rights reserved.
PII: S0301-4622(02)00144-8

transition observed [2,3]. Deviations of protein conformation from globular native to less compact, unfolded structures in those gel systems were first revealed through nuclear magnetic resonance (NMR) and Raman spectroscopies [1]. More recently, the dynamic polydispersed character of these viscoelastic matrices was clearly established through rheological experiments [4,5].

The small angle X-ray scattering (SAXS) technique [6] was first applied in the investigation of these gel-like systems at low lysozyme concentration conditions, where no gel formation is observed [6]. Results fitted a two-state equilibrium model, indicating a critical solvent concentration at TMU/water mass fraction, w_{TMU}, of 0.6, in which two populations of lysozyme are present in approximately equal amounts: one composed of globular proteins with radius of gyration $R_g \cong 16$ Å and the other of highly anisometric character with $R_g \cong 47$ Å. Such a critical concentration corresponds to that observed in the binary solvent alone (without protein), as the critical concentration where an inversion in the complex liquid microconfiguration takes place [1,4,5].

With the aim of investigating the features of the system in the high protein concentration regime, the present work is undertaken. Under these conditions, the system forms viscoelastic three-dimensional network of semi-solid character, displaying interference effects in the scattering curves for certain ranges of the binary TMU/water solvent composition. The results are compared with those obtained for the same lysozyme/water system in the absence of TMU, which does not present a sol–gel phase transition.

Understanding the behavior of proteins in nonconventional media can be of assistance in folding investigations. The distinctive behavior presented by protein domains in extraneous microenvironments may in principle provide insights into the complex interplay of forces acting in these macromolecular structures. In particular, proteins in organic media have been known to present peculiar structural features that affect their functionality, as in the case of certain enzymatic systems [7]. From a practical point of view, the possibility of developing malleable, semi-solid protein media, as in the case of the protein viscoelastic matrices presented in this work, may be also of potential interest in the biotechnological area.

2. Experimental

2.1. Materials and sample preparation

Hen egg white lysozyme was obtained product from Pharmacia. Tetramethylurea was purchased from Aldrich. Ultra-pure water (Elga System UHQ, 18 MΩ cm) was employed throughout. Lysozyme samples were prepared by careful dispersion of the protein in the binary mixtures. TMU mass fraction (w_{TMU}) in the binary solvents ranged from 0.6 to 0.9, in 0.1 intervals, for a fixed protein concentration of 0.50×10^{-2} mol dm^{-3}. Systems were manually homogenized and then left undisturbed until complete evolution of the sol–gel transition [4,5]. Under protein concentrations employed, viscoelastic lysozyme matrices started to form typically after 15 min, for $w_{TMU} = 0.9$. As protein is also being employed here as a probe for the binary mixture configurational transition, which has been previously characterized in the absence of electrolytes, pH buffering was intentionally not used at this stage. pH changes in the systems were, however, monitored throughout. For aqueous lysozyme samples, pH was 3.4. For lysozyme in TMU/water, pH increased from 3.5 to 4.0, for TMU mass fraction variation from 0.1 to 0.4, and from 5.0 to 5.9 for TMU mass fraction increasing in the range 0.5 to 0.9. Scattering data were collected after approximately 72 h from sample preparation, in order to allow the attainment of a steady state condition for the gels.

SAXS curves were obtained at the SAXS beamline of the Brazilian National Synchrotron Light Laboratory (LNLS), at room temperature (22 ± 1) °C, with radiation wavelength $\lambda = 1.608$ Å and sample-to-detector distance of 1008 mm. Samples were conditioned in sealed 1-mm-thick acrylic cells, with Mylar windows, perpendicular to the incident X-ray beam. The obtained curves (data collection of 15 min) were corrected for detector inhomogeneity (one-dimension position sensitive detector), sample's attenuation and background scatterings, using controls that consisted of TMU/water solutions in the appropriate concentration

for samples in the gel phase and water for lysozyme aqueous solution.

2.2. Data analysis

2.2.1. Basic equations

The small angle X-ray scattering is a powerful tool that yields information on the overall shape and size of biological macromolecules in solution. Its application is thus particularly useful in studying systems where large conformational changes take place, as in the process of protein folding/unfolding as well as in aggregation.

In the frame of the so-called two-phase model, monodisperse proteins in a dilute solution act as randomly oriented scattering particles of homogeneous electron density ρ, dispersed in a solvent with different homogeneous electron density ρ_0 [8]. In this condition, the excess X-ray scattering intensity is given by

$$I(q)=\gamma n_p(\Delta\rho)^2V^2P(q)S(q) \quad (1)$$

where γ is a factor related to the instrumental effects, n_p corresponds to the particle number density; $\Delta\rho=\rho-\rho_0$ is the electron density contrast between the scattering particle and the medium and V is the scattering particle volume. $P(q)$ in Eq. (1) is the normalized particle form factor ($P(0)=1$) and $S(q)$ is the interparticle interference factor ($q=(4\pi/\lambda)\sin\theta=$scattering vector and $2\theta=$scattering angle).

A Fourier transform connects $P(q)$, and hence $I(q)$ in the absence of interference effects on the scattering curves, to the distance distribution function $p(r)$, the probability of finding pair of small volume elements at a distance r within the entire volume of the scattering particle as [9]

$$p(r)=(1/2\pi^2)\int_0^\infty I(q)qr\sin(qr)dq \quad (2)$$

The behavior of $p(r)$ provides information about the shape of the scattering particle and $p(r)=0$ for $r=0$ and for distances larger than the object maximum dimension D_{max}. Moreover, the particle radius of gyration R_g is defined as [9]

$$R_g^2=\left(\int_0^{D_{max}}p(r)r^2dr\right)/\left(2\int_0^{D_{max}}p(r)dr\right) \quad (3)$$

In this work, we use the GNOM program [10] to calculate $p(r)$ in the gel phase at $w_{TMU}=0.9$, a condition in which $S(q)$ is not present in the scattering curve. We also make use of Kratky plot (i.e. $q^2I(q)$ vs. q) for this particular sample in order to detect folded/unfolded states [11–13]. For a globular protein, Kratky's plot displays a peak whose position depends on R_g. However, the graph tends to show a plateau when the protein assumes a completely unfolded, random-coil conformation.

For the other samples, where $S(q)$ is pronounced over the scattering curves, the protein's structural parameters are obtained by fitting the product $P(q)S(q)$ [Eq. (1)] to the experimental curve. The models for $P(q)$ and $S(q)$ used in this work are summarized below.

It should be remarked that it is possible to measure the intensity in absolute scale in a SAXS experiment (γ is determined) and, hence, to obtain direct information about the pre-factor $n_pV^2\Delta\rho^2$. However, in this work, an interpretation of such pre-factor would require taking into account the local densities of the segregated microphases directly in contact with the scattering particles, at each solvent composition. That is justified since microphase segregation of the binary mixture has been known to occur in TMU/water binary liquid systems as a function of solvent composition [1,3,14], being ultimately responsible for the evolution of the protein sol–gel transition itself [1–3]. A direct estimate of local microphases densities is, however, impaired by the very peculiar aspects of the complex TMU/water microconfigurational status, which may include an influence, as yet not estimated, of protein molecules in the high concentration regime on the binary solvent microdomain organization. Therefore, no quantitative interpretation of this pre-factor will be offered at this stage and $n_pV^2\Delta\rho^2$ will be used as a normalization factor in the fitting procedure to the experimental curves.

2.2.2. $P(q)$ and $S(q)$ modeling

Several algorithms have been developed to calculate $P(q)$ for low molecular weight proteins in water medium from known atomic structure [15–18]. In our case, however, we do not know, a

priori, how the protein conformation (and hence its shape and size) is affected by mixing an organic (TMU) solvent to the aqueous solution. Then, we decided to make use of a unified equation recently developed by G. Beaucage [19]. Such equation describes the scattering of polymers in solution in terms of R_g and boundary macromolecule/solvent interface properties, bringing together the Guinier and Porod laws, such that

$$P(q) \approx G\exp\left(\frac{-q^2R_g^2}{3}\right) + B\left[\frac{\left(\mathrm{erf}\left(qR_g/\sqrt{6}\right)\right)^3}{q}\right]^A \quad (4)$$

where G is the Guinier pre-factor [$n_p V^2 \Delta\rho^2$, Eq. (1)]; B is a pre-factor specific to the type of power-law scattering; A is the nature of the interface, characteristic of the power law in the Porod's region: ($A>4$, diffuse interface [20]; $A=4$, rigid interface; $4>A>3$, surface fractal; $A<3$, volume or mass fractal; $A=2$, Gaussian polymer); erf is the error function.

As far as we are aware, Beaucage's methodology has not been previously applied to analyze small angle scattering data from protein-containing systems. In our case, we use the approach given in Eq. (4) considering the protein as a biopolymer. In order to check the validity and limitations of Eq. (4) for the studied system, Fig. 1 shows the best fitting of Eq. (4) to the theoretical lysozyme form factor $P(q)$ generated from its native structure (EC 3.2.1.17) [21] by using Crysol [18]. The fitting parameters resulted to be $R_g=16$ Å and $A=4$, in very good agreement with the value of radius of gyration calculated from the lysozyme crystallographic monomeric globular shape ($R_g=15\pm1$ Å) [18] with a well-defined interface.

However, unfolded proteins can have a fractal dimension that characterizes the topological nature of the conformation of the polypeptide chains [22,23], justifying the use of Eq. (4) to investigate changes in the macromolecule interface features induced by the presence of the organic solvent. In this context, B and G in Eq. (4) are correlated for mass fractals through [24,25]

$$B=\left(\frac{GA}{R_g^A}\right)\Gamma\left(\frac{A}{2}\right) \quad (5)$$

where Γ is the gamma function.

Of course, $A<4$ can also be related to polydisperse systems [26]. These two possibilities (systems composed of different protein states and/or macromolecules displaying fractal character) will be evaluated in the data discussion.

Further, considering that for $A<3$ Eq. (5) applies, we made use of the constraint between B and G, greatly improving the convergence in the modeling process, when it was the case. Again, as explained above, G includes a normalization factor to the experimental data.

As to the interference contribution, simulation of $S(q)$ has been extensively developed in liquid state physics. Models and numerical methods based on statistical mechanics have recently been extended to proteins in solution [27–29]. In particular, investigation about the interference function has been performed on a series of SAXS data recorded on lysozyme in a water system [30] as a function of pH, salt concentration, salt type and temperature. The interaction potentials and the numerical treatment make use of the so-called DLVO model that includes hard core, coulombic electrostatic interactions and attractive van der Waal's forces, provided that the globular protein remained compact in the data analysis. In our case, the protein undergoes a shape transformation under the influence of the binary organic/water environment, as already shown at low protein concentrations [6] and presented below for high lysozyme concentration regime. Then, our analysis will be simply based on the modifications occurring in the mean distances between the scattering particles as the system evolves from a Newtonian to a viscoelastic fluid, without taking explicitly into account the interaction potentials that control the macromolecular distribution in solution. In this context, we make use of a semi-empirical function for $S(q)$ that describes correlations of colloidal particles (or particle domains) as [8,31].

$$S(q)=\frac{1}{1+k\varphi(qd)} \quad (6)$$

where $\varphi(qd)$ is the 'spherical form' factor for

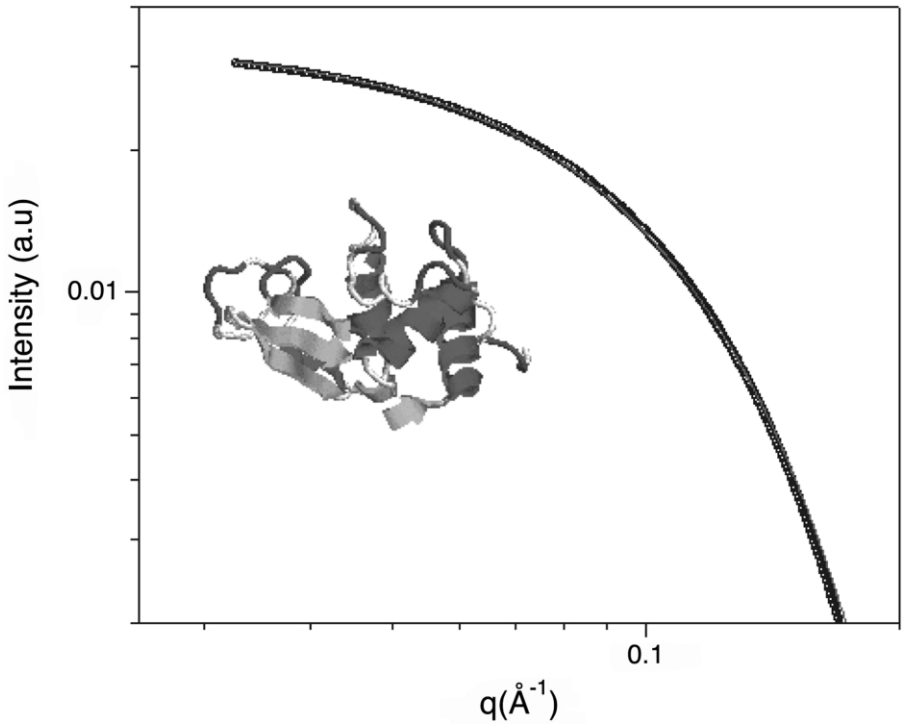

Fig. 1. Theoretical lysozyme form factor $P(q)$ curve generated from its native structure (EC 3.2.1.17) [21] using Crysol [18] (○) and best fitting according to Eq. (4) (–).

structural correlations occurring at an average radial distance, d; and k is the degree of correlation $(0<k<6)$. The latter value corresponds to maximum packing condition.

The spherical form factor $\varphi(qd)$ is explicitly expressed as:

$$\varphi(qd)=3(\sin(qd)-qd\cos(qd))/(qd)^3 \quad (7)$$

3. Results and discussion

SAXS curves obtained for lysozyme aqueous solution and for the protein dispersed in water/TMU mixtures, in the $w_{TMU}=0.6$–0.9 solvent concentration range are presented in Fig. 2. In all cases, lysozyme concentration was kept constant and equal to 0.50×10^{-2} mol dm^{-3}. That was found to be the threshold protein concentration for the onset of a rheological transition that turns Newtonian lysozyme solutions into semi-solid viscoelastic matrices [1].

Striking differences between the scattering curve profiles observed for lysozyme in water and for the protein in the organic/aqueous media, in the concentration range investigated, can be observed in Fig. 2. Interference effects are present in the scattering curves for the protein both in aqueous solution and in TMU/water media, at the $w_{TMU}=0.6$–0.8 concentration range. At $w_{TMU}=0.9$, however, the interference effect completely disappears. Also, the interference peak is located at a significantly lower region of q values ($q\approx0.03$ Å^{-1} vs. $q\approx0.08$ Å^{-1}, for lysozyme in TMU/water and aqueous solutions, respectively), indicating that the average distance between the centers of mass of scattering particles is much larger in TMU/water media than in aqueous solution. Under a rheological point of view, systems in the TMU/water media are viscoelastic, with gel-like appearance [1,4], whereas lysozyme aqueous solutions comprise Newtonian fluids.

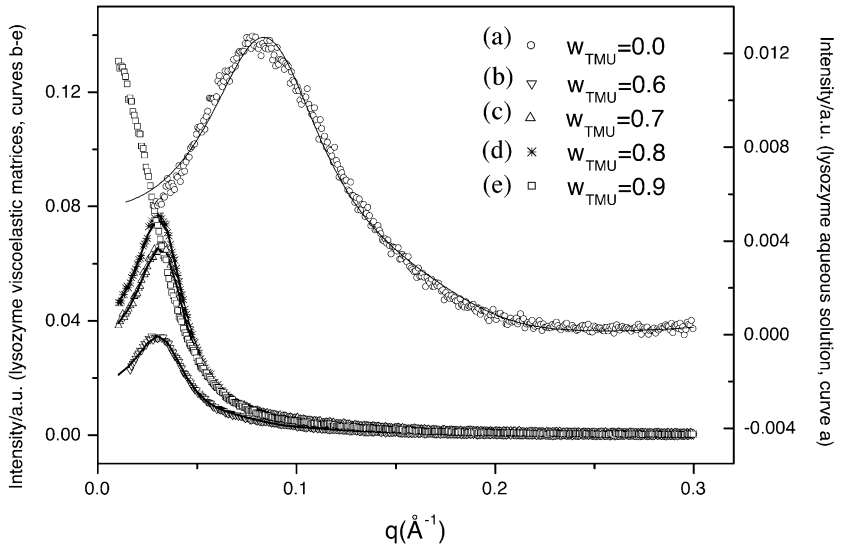

Fig. 2. SAXS curves for lysozyme in aqueous solution (curve a) and in TMU/water for increasing w_{TMU} in the binary solvent (curves b–e, comprising viscoelastic semi-solid matrices), all at protein concentration 0.50×10^{-2} mol dm^{-3}. Solid lines refer to best fittings of the $P(q)S(q)$ product to the experimental curves (curves a–d). Output modeling parameters are shown in Table 1. Curve fitting for curve e is shown in Fig. 3.

There is a considerable gain of intensity (approx. four times) when the system evolves from Newtonian (protein in water solution) to viscoelastic behavior at $w_{TMU}=0.6$. That is the critical solvent composition where the binary solvent microconfigurational inversion has been found to take place [1–3]. Changes in local densities of the microphases are therefore expected to occur and that may lead to differences in $\Delta\rho$ [Eq. (1)]) and, hence, in intensity. Increasing intensities of the SAXS curves at $w_{TMU}=0.7$ and $w_{TMU}=0.8$ (Fig. 2) can also be assigned to this effect, since the local densities of the solvent segregated microphases in contact with the macromolecules must change as a function of TMU/water ratio [1,3,14].

Best fittings to the scattering curves making use of Eq. (1) and Eqs. (4)–(6) are also presented in Fig. 2 for lysozyme in water and in TMU/water binary mixtures, in the concentration range of $w_{TMU}=0.6$–0.8. Table 1 shows the best parameters extracted from the fitting procedures. For lysozyme in aqueous solution, a radius of gyration $R_g=14$ Å was observed, which is consistent with the calculated value from lysozyme crystallographic

Table 1
Output parameters from the fitting of SAXS curves with $P(q)S(q)$, for lysozyme/water and lysozyme/water/TMU systems[a]

[Lysozyme]	0.5×10^{-2} mol dm^{-3}				
w_{TMU}	0	0.6	0.7	0.8	0.9
R_g (Å)	14.0±0.1	44±3	43.5±1.5	43.5±2.0	49.0±0.5
d (Å)	62.0±0.3	156±3	154±1	156±2	–
k	2.50±0.05	2.0±0.2	2.0±0.2	2.0±0.2	–
A	4.0±0.2	2.4±0.1	2.7±0.1	2.8±0.1	2.8±0.1

[a] $P(q)$ parameters [Eq. (4)] are the scattering particle radius of gyration R_g (Å) and the power factor A (adimensional); d (Å) and k (adimensional) refer to the average distance between scattering particles and to the correlation degree, for the $S(q)$ function (Eq. (6)), respectively.

structure [18]. Parameter A resulted in values of approximately 4 (Table 1). This indicates an intense change in electronic density at the protein surface, indicating a sharp interface. Interparticle correlation, as estimated through parameter k, is 2.5, which is slightly greater than k values observed for lysozyme in TMU/water. The average distance between particles (d) for lysozyme in water was 62 Å, only slightly lower than that obtained by Minezaki et al. [32] directly from the interference peak position ($d \approx 2\pi/q_{peak}$).

The most prominent observation is the drastic change in scattering particle radius of gyration R_g from 14 Å in water to circa 44 Å in TMU/water (for $w_{TMU}=0.6$, 0.7 and 0.8, and 0.50×10^{-2} mol dm^{-3} lysozyme concentration), accompanied by an increase of the mean distance between the scattering units from 62 Å to approximately 155 Å (Table 1). It should be noted, as already indicated, that such changes correspond macroscopically to the formation of semi-solid matrices of viscoelastic character. The degree of correlation $k \approx 2$ (Table 1) indicates that systems are not in a condition of maximum packing, which is compatible with the observed great flexibility of such network structures, as expressed by their large linear viscoelastic regions verified in strain amplitude tests [4]. The close proximity of the R_g value ($R_g=44$ Å), found for the scattering particles in the lysozyme viscoelastic matrices, to that obtained [6] for aqueous solutions of lysozyme in the diluted regime (0.30×10^{-3} mol dm^{-3}), at $w_{TMU}=0.7$, where systems are Newtonian fluids (no gel character), is noteworthy. That confirms previous observations [1–3] according to which protein conformational transition seems to be totally induced by the organic/aqueous solvent, in a way that is independent from the protein concentration and consequently from the intermolecular contacts leading to gel formation. Besides, the parameter A presented values between 2 and 3 (Table 1), indicating either fractal character for the scattering particles in the gel matrices or sample polydispersion, or both.

Since rheological studies on these systems have clearly pointed out their polydispersed character, with two dynamically very distinct populations [4], the exclusive assignment of parameter A to fractality cannot, therefore, be made unequivocally. However, it is important to note that the rheological measurements have in fact identified two distinct *dynamical* populations, which may not have a direct correlation with morphologically distinct protein molecular populations, but rather with associations between unfolded protein molecules and the apolar continuum of the organic solvent microdomains. As will be seen, a simple or direct correlation between dynamical role and protein conformational status is not easily acknowledged for those systems. That aspect will be brought back into discussion later in this text.

The disappearance of the interference function at $w_{TMU}=0.9$, reflecting the absence of correlation between the scattering centers is intriguing (Figs. 2 and 3). It is interesting to note that the SAXS curve profiles, for all TMU mass fractions, are very similar to that obtained at $w_{TMU}=0.9$ after the interference peak (Fig. 2). That indicates that the scattering particles in the protein gels are likely to have similar shapes, irrespective of the occurrence of the interference effect. In fact, dynamical rheological measurements performed in these systems [4] indicate the maintenance of the linear viscoelastic region, independently of solvent composition, implying that one same network general structure is present in the matrices, which is in agreement with the scattering findings described in this work.

Transient rheological assays, however, indicate strikingly different dynamical characteristic for the gels developed at $w_{TMU}=0.6$, 0.7, 0.8 and 0.9, with very distinct viscous and elastic contributions in each case [4]. Those studies have also indicated polydispersion for all gel samples assayed, with curves fitting double exponential functions. In all cases, systems comprised two dynamic populations, with relaxations differing in approximately one order of magnitude from each other, for each solvent concentration (w_{TMU}). In the gel at $w_{TMU}=0.9$, however, the elastic contribution was found to be major (amounting to 92%), with gel behavior approaching that of a perfectly elastic solid. This is in accordance with the SAXS results presented here for the gel at that solvent concentration ($w_{TMU}=0.9$), since the absence of interference is likely to be indicating a matrix condition where

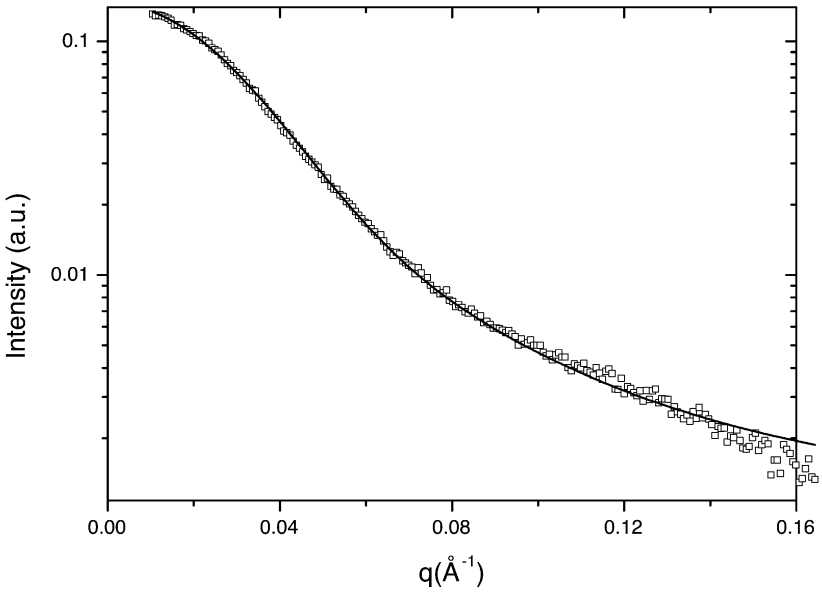

Fig. 3. SAXS curve of lysozyme/water/TMU at $w_{TMU}=0.9$, with protein concentration equal to 0.50×10^{-2} mol dm^{-3}. Solid line represents the best fitting of the form function $P(q)$ to experimental data. Output modeling parameters are shown in Table 1.

lysozyme molecules are completely intermingled in the TMU continuum. Such a condition would be expected to enhance the elastic character of the gel, as verified [4]. For gels at $w_{TMU}=0.6$, 0.7 and 0.8, however, the viscous contributions are significant, amounting to 60%, 40% and 21%, respectively [5]. For these systems, nevertheless, SAXS results indicate very similar matrix morphologies, with scattering particle not very distinct from that found at $w_{TMU}=0.9$. Those apparently conflicting results could be understood if one assigns the elastic contribution in the matrices, revealed in rheological experiments, predominantly to the apolar extended domains, comprising the TMU continuum and intermingled unfolded protein molecules; and the viscous contribution mainly to the dispersed aqueous microdomains in the lattice. Such assignments are in accordance with the maintenance of both the network morphology (according to the SAXS analysis in this work) and the linear viscoelastic region (according to rheological evidence [4]).

Fig. 3 shows the fitting to the SAXS curve obtained at $w_{TMU}=0.9$, using $P(q)$ form function [Eq. (4)]. As can be seen in Fig. 3 and from the fitting parameters in Table 1, the scattering units at $w_{TMU}=0.9$ also display the A parameter in the range ascribed to mass fractal character ($A=2.8$), although sample polydispersion, as previously pointed out, could as well respond for that value. However, since polydispersion is much less relevant at that solvent concentration, it seems very likely that the fractal character has, in fact, an important role in parameter A. The radius of gyration is equal to 49 Å, which is slightly larger than those observed for $w_{TMU}=0.6$–0.8, and much larger than that of the native protein ($R_g=14$ Å). Fig. 4a presents the distance distribution function $p(r)$, calculated through the GNOM program, which indicates $D_{max}=150$ Å and $R_g=49$ Å. With the aim of verifying if that indicates extensive protein unfolding, we analyzed data through the Kratky plot, where the characteristic profile verified for the native protein is included for comparison (Fig. 4b). The observed peak in the modified protein curve indicates that the scattering particle is not totally unfolded. Complete unfolding would actually not be expected, due to particularities of lysozyme covalent structure with four intramolecular disulfide linkages. However, the extent of

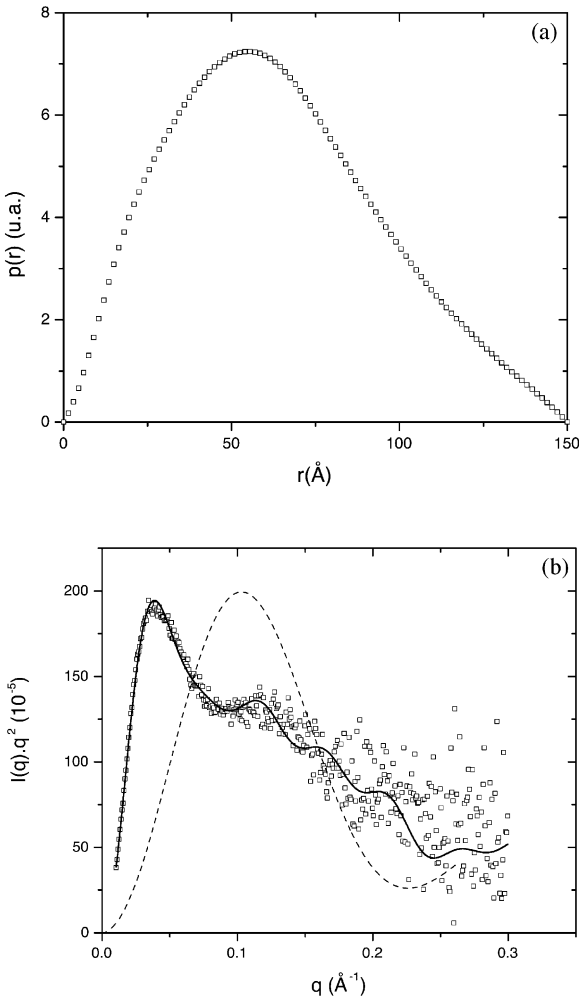

Fig. 4. Lysozyme/water/TMU at $w_{TMU}=0.9$, with protein concentration equal to 0.50×10^{-2} mol dm^{-3}: (a) $p(r)$ distance distribution function; (b) Kratky plot (open symbols) and theoretical scattering function corresponding to p(r) (–); Kratky plot corresponding to the scattering of lysozyme native conformation (normalized) is also included (- - -) for comparison.

unfolding is certainly more extensive in this case than in the presence of usual denaturants, like urea ($R_g=22$ Å for lysozyme in 8 M urea [33], for instance). That has been further supported by the observation of very distinctive rheological and spectroscopic behavior of lysozyme in TMU/water as compared to that in concentrated urea [1]. Raman scattering has also indicated that secondary structures are considerably diminished but still present in viscoelastic lysozyme, although in the organic–aqueous media where that was found, such structures typically bear a rather loose, less-tightly packed conformation, of a non-orthodox character [1].

The maximum particle dimension D_{max} at $w_{TMU}=0.9$ is of the order of the mean distance d between the scattering particles at $w_{TMU}=0.8$. A small increase in R_g at $w_{TMU}=0.9$ relative to its condition in the previous lower organic solvent concentration may lead to a complete lysozyme interdigitation with the apolar prevailing medium as already pointed out, resulting in the loss of the interparticle interference effect, as observed.

Relevant experimental data on the many physico-chemical aspects of TMU non-ideal behavior, and that of its aqueous solutions, have been put forth in the literature in the last decades [14,34–37]. TMU/water mixtures display very pronounced deviations from ideal behavior. They constitute, in fact, microheterogeneous systems and that is of critical interest in the context of this work, since strikingly distinct flow behavior is observed for proteins dispersed in these media, as a function of the binary solvent composition [1,4]. It has been known that these binary systems play a water structuring role up to a molar concentration of 0.2 mol/dm^3 at room temperature, whereas acting as water destructuring at higher concentrations. That creates anomalies in water diffusion: diffusion coefficients determined by the SANS technique for water in TMU are significantly lower than in pure water, whereas TMU diffusion coefficients are kept practically constant [14,34]. A cage model, commonly accepted for clathrates, is proposed to explain the data [35]. Density, viscosity and absorption maxima for aqueous TMU solutions are observed at approximately 0.2 molar fraction (which corresponds to $w_{TMU}=0.6$, coincidently, the threshold concentration for lysozyme viscoelastic transition), whereas compressibility excess values display minima at these same concentrations [37]. Partial molar volumes for TMU and water in their mutual mixtures reveal the occurrence of remarkable deviations in that region. An inversion in the microdomain configuration has been proposed to occur in TMU/water mixtures at that critical solvent composition and to consti-

tute the driving force for the viscoelastic protein transition observed [1–3].

Although a general trend for the protein transition observed has been proposed in previous studies [1–3], the detailed mechanism through which the binary mixture transition affects the unfolded protein solvation is still an open question in many of its aspects, particularly taking into account the fact the solvent configurational status may show a dependence on the protein's extent of unfolding. In this respect, the present study brings important new experimental support to the overall picture, offering a morphological description of the unfolded proteins in the network structure, which is compatible with the dynamical characteristics displayed by these systems.

4. Conclusions

Drastic morphological changes were found to be involved in the sol–gel transition undergone by lysozyme in TMU/water media, as characterized in this work through the SAXS technique. The analysis of SAXS curves in their form and interference factors revealed an increase in scattering particle radius of gyration R_g from 14 Å for the protein in water to circa 44 Å in the viscoelastic matrices. The changes also comprised an increase of the mean distance between the scattering units from 62 Å to approximately 155 Å. At $w_{TMU}=0.9$, particle D_{max} was of the order of interparticle distance such that a small increase in R_g (to $R_g=49$ Å) lead to interdigitation with the apolar matrix domains, with consequent loss of the interference effect, consistently present at $0.6 \leq w_{TMU} \leq 0.8$. Particle interface evolved from sharp character (in water) to mass fractal in the matrices, although sample polydispersion could possibly have some contribution to that. Despite significant shape distortions, non-negligible globular character is still recognizable in lysozyme molecules after the sol–gel transition, which is assigned to the limit imposed by lysozyme disulfide bridges.

Acknowledgments

We thank the National Laboratory of Synchrotron Light (LNLS, Campinas, Brazil (Proc. 644/00)) for the use of their facilities. This work is part of a project by one of the authors (E.P.G. Arêas), supported by FAPESP (Brazil). It contains part of the work developed in the Master's thesis of M.A. da Silva, to whom a CNPq (Brazil) scholarship has been granted. R. Itri and E.P.G. Arêas are grateful to CNPq for the grant of research fellowships. R. Itri also thanks support from FAPESP and CAPES.

References

[1] E.P.G. Arêas, J.A.G. Arêas, J. Hamburger, W.L. Peticolas, P.S. Santos, On the high viscosity of lysozyme aqueous solution induced by some organic solvents, J. Coll. Interface Sci. 180 (1996) 578–589.
[2] E.P.G. Arêas, H.H.A. Menezes, P.S. Santos, J.A.G. Arêas, Hydrodynamic, optical and spectroscopic studies of some organic-aqueous binary systems, J. Mol. Liquids 79 (1999) 45–58.
[3] E.P.G. Arêas, J.A.G. Arêas, Mesoscopic segregation in binary liquid solutions: application of a model for block copolymers to non-macromolecular systems, J. Molec. Structure (Theochem.) 464 (1999) 199–209.
[4] M.A. da Silva, E.P.G. Arêas, Rheological study on lysozyme/tetramethylurea viscoelastic matrices, Biophys. Chem. 99 (2002) 129–141.
[5] M.A. da Silva, E.P.G. Arêas, Rheological studies of protein viscoelastic networks in organic/aqueous media, Biophys. J. 82 (2002) 324a–324a.
[6] V. Castelletto, E.P.G. Arêas, J.A.G. Arêas, A.F. Craievich, Effects of tetramethylurea on the tertiary structure of lysozyme in water, J. Chem. Physics 109 (1998) 6133–6139.
[7] A.M. Klibanov, Improving enzymes by using them in organic solvents, Nature 409 (2001) 241–246.
[8] A. Guinier, G. Fournet, Small Angle Scattering of X-Rays, Wiley, New York, 1955.
[9] O. Glatter, O. Kratky, Small Angle X-ray Scattering, Academic Press, London, 1982.
[10] A.V. Semenyuk, D.I. Svergun, GNOM—a program package for small angle scattering data processing, J. Appl. Crystallogr. 24 (1991) 537–540.
[11] G.V. Semisotnov, H. Kihara, N.V. Kotova, et al., Protein globularization during folding. A study by synchrotron small angle X ray scattering, J. Mol. Biol. 262 (1996) 559–574.
[12] D.J. Segel, A.L. Fink, K.O. Hodgson, S. Doniach, Protein denaturation: a small angle X ray scattering study of the ensemble of unfolded states of cytochrome c, Biochemistry 37 (1998) 12443–12451.
[13] S. Cinelli, F. Spinozzi, R. Itri, et al., Structural characterization of the pH denatured states of ferrycytochrome-c synchrotron small angle X ray scattering, Biophys. J. 81 (2001) 3522–3533.

[14] P. Belletato, L.C.G. Freitas, E.P.G. Arêas, P.S. Santos, Computer simulation of liquid tetramethylurea and its aqueous solution, Phys. Chem. Chem. Phys. 1 (1999) 4769–4776.
[15] C.A. Pickover, D.M. Engelmann, On the interpretation and prediction of X ray scattering profiles of biomolecules in solution, Biopolymers 21 (1982) 817–831.
[16] M.Y. Pavlov, B.A. Fedorov, Improved technique for calculating X ray scattering intensity of biopolymers in solution—evaluation of the form, volume, and surface of a particle, Biopolymers 22 (1983) 1507–1522.
[17] E.E. Lattman, Rapid calculation of the solution scattering profile from a macromolecule of known structure, Proteins 5 (1989) 149–155.
[18] D. Svergun, C. Barberato, M.J.H. Koch, CRYSOL—a program to evaluate X ray solution scattering of biological macromolecules from atomic coordinates, J. Appl. Crystallogr. 28 (1995) 768–773.
[19] G. Beaucage, Approximations leading to a unified exponential power-law approach to small-angle scattering, J. Appl. Crystallogr. 28 (1995) 717–728.
[20] J.T. Koberstein, B. Morra, R.S. Stein, Determination of diffuse boundary thicknesses of polymers by small angle X ray scattering, J. Appl. Crystallogr. 13 (1980) 34–45.
[21] http://www.rcsb.org/pdb/
[22] S.H. Chen, J. Teixeira, Structure and fractal dimension of protein-detergent complexes, Phys. Rev. Lett. 57 (1986) 2583–2586.
[23] X.H. Guo, N.M. Zhao, S.H. Chen, J. Teixeira, Small angle neutron scattering study of the structure of protein detergent complexes, Biopolymers 29 (1990) 335–346.
[24] G. Beaucage, D.W. Schaefer, Structural studies of complex-systems using small-angle scattering—a unified Guinier power-law approach, J. Non-Cryst. Solids 172 (1994) 797–805.
[25] G. Beaucage, Small-angle scattering from polymeric mass fractals of arbitrary mass fractal dimension, J. Appl. Crystallogr. 29 (1996) 134–146.
[26] P.W. Schmidt, Interpretation of small angle scattering curves proportional to a negative power of the scattering vector, J. Appl. Crystallogr. 15 (1982) 567–569.
[27] A. Lomakin, N. Asherie, G.B. Benedek, Monte Carlo study of phase separation in aqueous protein solutions, J. Chem. Phys. 104 (1996) 1646–1656.
[28] M. Malfois, F. Bonneté, L. Belloni, A. Tardieu, A model of attractive interactions to account for fluid-fluid phase separation of protein solution, J. Chem. Phys 105 (1996) 3290–3300.
[29] F. Bonneté, M. Malfois, S. Finet, A. Tardieu, S. Lafont, S. Veesler, Different tools to study interaction potentials in gamma-crystallin solutions: relevance to crystal growth, Acta Crystallogr. D 53 (1997) 438–447.
[30] A. Tardieu, A. le Verge, M. Malfois, F. Bonneté, S. Finet, M. Riès-Kautt, L. Belloni, Proteins in solution: from X-ray scattering intensities to interaction potentials, J. Cryst. Growth 196 (1999) 193–203.
[31] G. Beaucage, T.A. Ulibarri, E.P. Black, D.W. Schaefer, Multiple size scale structures in silica-siloxane composite studied by small angle scattering, Hybrid organic-inorganic composites, ACS Symposium Series, 585, 1995, pp. 97–111.
[32] Y. Minezaki, N. Niimura, M. Ataka, T. Katsura, Small angle neutron scattering from lysozyme solutions in unsaturated and supersaturated states (SANS from lysozyme solutions), Biophys. Chem. 58 (1996) 355–363.
[33] L.L. Chen, K.O. Hodgson, S. Doniach, A lysozyme folding intermediate revealed by solution X ray scattering, J. Mol. Biol. 261 (1996) 658–671.
[34] L. Cser, G. Jancsó, R. Papoular, T. Grósz, Anomalous diffusion of tetramethylurea (TMU) in aqueous solution, Physica B 156 (1989) 145–147.
[35] L. Cser, B. Farago, T. Grosz, G. Jancsó, E. Ostanevich, M. Yu, Structure and dynamics of aqueous solutions of tetramethylurea, Physica B 180 (1992) 848–850.
[36] L. Cser, T. Grósz, G. Jancsó, G. Kali, The nature of the interaction of tetramethylurea in various solvents, Physica B 234 (1997) 349–350.
[37] K. Sasaki, K. Arakawa, Ultrasonic and thermodynamic studies on the aqueous solutions of tetramethylurea, Bull. Chem. Soc. Jpn. 46 (1973) 2738–2741.